

Fig. 2 Bottom view of square tip at 400 rpm and 10° pitch angle.

solution which was sprayed onto the tip. The ammonia vapor reacted with the diazonium salt solution and left dark traces on the surface indicative of the local flow direction. Photographs were taken of the tip following a test. The model rotor had a diameter of approximately 8 ft and had a 9-in. chord. The tests were conducted at 400 rpm resulting in a tip Reynolds number of 8×10^5 . Tests at rotor blade pitch angles from 0° to 16° in 2° increments were performed.

Results with Square Tip

Figures 1 and 2 show a typical set of flow traces on the upper, end, and lower surfaces of the square tip at 400 rpm and 10° pitch angle. The traces on the upper surface reveal that the flow direction changes from inward to outward at the seventh hole from the leading edge. Also, the traces on the end of the tip indicate that the flow direction changes from upward to downward at the same distance back from the leading edge. These sudden changes in flow direction on the tip indicate the point of vortex inception. The flow traces on the lower surface indicate outflow over most of the blade except near the trailing edge where the flow moves in a chordwise direction.

Figure 3 depicts schematically the general flow pattern around the square tip. Three regions can be discerned, namely the first ~30% chord, ~30% to ~70% chord, and finally the last ~30% chord. In the first region, the flow rolls up around the tip and spills over onto the upper surface because of the strong pressure gradient which exists between the upper and lower surfaces. In the second region, the magnitude of the flow from the lower surface to the upper surface reaches a higher level and results in the formation of secondary vortices on the end and top surfaces of the tip as shown in Sec. B-B. The local direction of the flow within

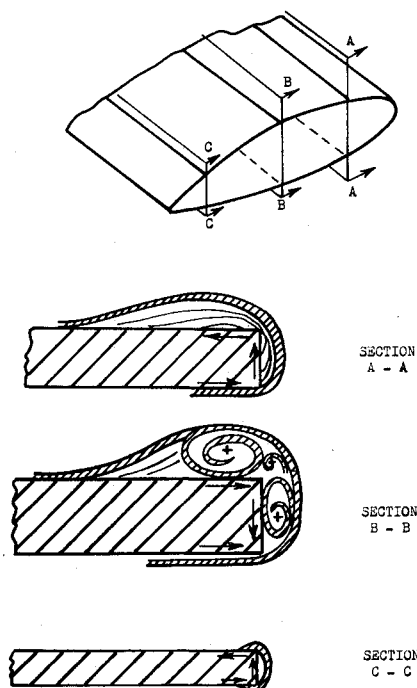


Fig. 3 Sketch of flow patterns around square tip.

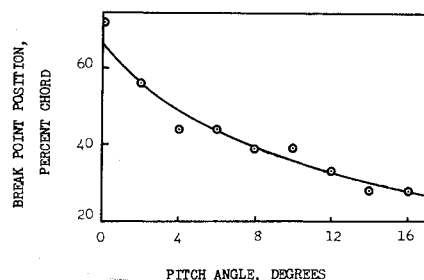


Fig. 4 Point at which traces change direction from inward to outward on upper surface of square tip vs pitch angle.

these vortices accounts for the outward and downward direction of the traces in these regions of the tip. The nature of the flow pattern in the last region is not as clearly defined, but some upward flow is indicated on the end of the tip from Figs. 1 and 2, and is shown in Sec. C-C.

It was found that the point at which the flow direction suddenly changes, i.e., the point of vortex inception, was a strong function of blade pitch angle. From examination of traces, the break point position, i.e., the point at which the traces turned from inward to outward, was determined and plotted as a function of pitch angle in Fig. 4. Figure 4 shows that the point of inception of the tip vortex varies from approximately 30% chord at 16° pitch angle to approximately 70% chord at 0° pitch angle.

The flow patterns that were found to exist on the rotor blade tips may also exist on the tips of regular wings. The ammonia trace technique utilized in these tests may prove useful in any such investigation of fixed wing tips as well as studying a number of surface flows on aircraft such as at inlet regions.

Real Gas Effects in Compressors for Aircraft Gas Turbines

ALLEN E. FUHS*

Naval Postgraduate School, Monterey, Calif.

THE trend to higher and higher pressure ratios in aircraft gas turbines leads to higher exit temperatures from the compressor. The vibrational degrees of freedom of oxygen begin to be thermally excited resulting in a decrease of the ratio of specific heats. The contribution of vibrational degrees of freedom to the heat capacity at constant volume is

$$C_{V,VIB}/R = [(\theta_V/2T)/\sinh(\theta_V/2T)]^2 \quad (1)$$

Equation (1) is based on the assumption of a harmonic oscillator. For oxygen the characteristic vibrational temperature

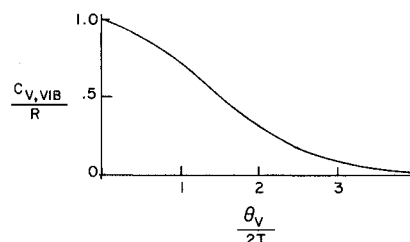


Fig. 1 Vibrational contribution to heat capacity.

Received March 17, 1971. This work was sponsored by the Eustis Directorate, U.S. Army Mobility Research and Development Laboratory, Ft. Eustis, Va.

* Professor, Department of Aeronautics. Associate Fellow AIAA.

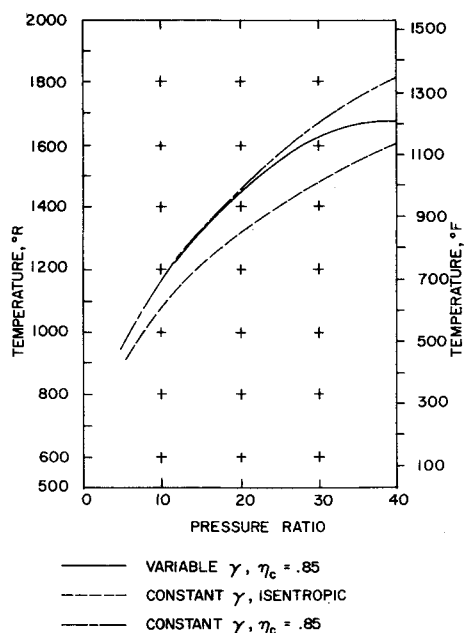


Fig. 2 Compressor exit temperature vs pressure ratio; inlet $T_T = 300^\circ\text{K}$.

θ_V is 2230°K . A graph of Eq. (1) is given in Fig. 1. It is apparent that when $\theta_V/2T = 3$, the vibration is about 10% excited. This occurs at 372°K or about 250°F . At 1660°F vibrational degrees of freedom in oxygen are 72% excited.

Compressor efficiency η_c is usually defined as

$$\eta_c = [\pi_c^{(\gamma-1)/\gamma} - 1]/(\tau_c - 1) \quad (2)$$

where π_c is stagnation pressure ratio and τ_c , the stagnation temperature ratio of the compressor. When real gas effects occur, a reasonable extension of the definition is

$$\eta_c = [\pi_c^{(\gamma-1)/\gamma} - 1]/(h_c - 1) \quad (3)$$

where γ is evaluated at the compressor inlet conditions and the symbol h_c represents the ratio of stagnation enthalpies.

Figure 2 is a plot of compressor exit temperature as a function of pressure ratio. Inlet stagnation temperature was taken as 300°K . The Mollier diagram for air from Little's report¹ was used to find exit values with variable γ . Notice that for pressure ratios to 30, the influence of variable γ is very slight. However, at 40, an error in temperature of about 10% results assuming constant γ .

It has long been recognized that variable γ is essential for describing processes in the hot section of the engine. For low pressure ratio engines, an assumption of constant γ for the compressor has been adequate. As seen in Fig. 2, for $\pi_c > 30$, proper analysis requires a variable γ .

In order to point out the significance of Fig. 2, a few aspects of compressor technology will be considered. Some instruments measure temperature; others measure enthalpy. Precision compressor testing at high π_c requires careful selection of instrumentation. Furthermore, interpretation of performance data should include enthalpy. Compressor efficiency based on τ_c is obviously more favorable than η_c based on h_c . Equation (3) yields a valid representation of over-all compressor losses. The compressor discharge air is used to cool the turbine blades. Cooling analysis and testing need to be based on compressor discharge enthalpy rather than temperature when $\pi_c > 30$. Current practice is to report cooling data in terms of temperature.² Transport properties, e.g., thermal conductivity, and dimensionless groups formed from transport properties, e.g., Prandtl number, change significantly when internal degrees of freedom are excited.³ A new approach for making point temperature measurements with fast time response is to use Raman scattering. Widhoff and

Lederman⁴ have demonstrated use of Raman scattering to measure species concentration. An extension of this approach will yield temperature. Above π_c of 30, the experimentalist has the choice of using Stokes or anti-Stokes vibrational bands to ascertain temperature. Finally, if one wants to understand combustion kinetics from a fundamental point of view, the presence of vibrationally excited O_2 in the combustor inlet is important. High pressure ratios are here today, e.g., JT9D has $\pi_c = 24.5$. The trend is to higher values. Real gas effects will become a factor to consider.

References

- Little, W. J., "Mollier Chart for Air," AEDC-TDR-63-190, Sept. 1963, von Kármán Gas Dynamics Facility, Arnold Engineering Development Center.
- "AGARD Conference Proceedings," *High Temperature Turbines*, No. 73, Sept. 1970.
- Hirschfelder, J. O., Curtiss, C. F., and Bird, R. B., *Molecular Theory of Gases and Liquids*, Wiley, New York, 1954.
- Widhoff, G. F. and Lederman, S., "Species Concentration Measurements Utilizing Raman Scattering of a Laser Beam," *AIAA Journal*, Vol. 9, No. 2, Feb. 1971, pp. 309-316.

Pulsed Air Gust Generator

JOSEPH BICKNELL*

Texas A&M University, College Station, Texas

Nomenclature

a	= speed of sound
A_j	= discharge area of all jet nozzles
A_t	= tunnel test section area
K	= $\omega/a\beta^2$
\dot{m}	= mass flow rate of all nozzles
\dot{m}_0	= twice the time average \dot{m}
M	= Mach number
p	= ambient absolute pressure
Δp	= pressure perturbation
R	= $[(x - \xi)^2 + (y - \eta)^2 + (z - \zeta)^2]^{1/2}$
t	= time
U	= average axial velocity
ΔU	= axial perturbation
V_j	= discharge velocity of jet nozzle
x, y, z	= coordinates of point in tunnel
β	= $(1 - M^2)^{1/2}$
γ	= ratio of specific heats
ρ	= mass density
ϕ	= velocity potential
ω	= circular frequency, rad/sec
ξ, η, ζ	= coordinates of point source

VARIOUS methods have been developed and used to produce oscillating airflows as tools for research on unsteady aerodynamics. Examples are oscillating wall mounted airfoils to produce lateral disturbances, and rotating shutters to produce longitudinal waves.¹ Thomas² carried out pilot testing on an array of jets downstream of the test section arranged to blow cyclically with time either upstream or downstream. This report concerns the calibration tests of an improved apparatus installed in a larger wind tunnel.

Presented as Paper 71-281 at the AIAA 6th Aerodynamic Testing Conference, Albuquerque, New Mexico, March 10-12, 1971; submitted April 1, 1971; revision received June 1, 1971. Early development of the pulsed air gust generator was sponsored by NASA, Langley Research Center. Later work was supported by the U.S. Army Research Office, Durham, under Themis Contract DAHCO4-69-0015.

Index Category: Nonsteady Aerodynamics.

* Visiting Professor, Aerospace Engineering Department. Member AIAA.